

Research

Improved security of medical images using DWT–SVD watermarking mechanisms based on firefly Photinus search algorithm

Waleed Alomoush¹ · Osama A. Khashan² · Ayat Alrosan¹ · Rafat Damseh³ · Mohammad Alshinwan⁴ · Alaa Ali Abd-Alrazaq⁵ · Mohanad A. Deif⁶

Received: 5 December 2023 / Accepted: 27 June 2024

Published online: 03 July 2024

© The Author(s) 2024 [OPEN](#)

Abstract

Security is the primary concern in the transmission of medical images, as it involves sensitive patient information. This study introduces an optimized watermarking approach, constructed using discrete wavelet transform and singular value decomposition. The Low-level frequency bands (LL3) sub-band singular values of the host image were embedded with the singular values of a binary watermark using multiple scaling factors. These MSFs were optimized using a recently proposed firefly Photinus algorithm to balance robustness and imperceptibility. The proposed method was applied to various images, including computed tomography images, where the visual quality of the signed and attacked images was evaluated by peak signal-to-noise ratio (PSNR) and normalized cross-correlation. The performance of the proposed algorithm demonstrates significant improvements in the embedding and extraction processes, showing an enhancement in the balance between robustness and imperceptibility, with a PSNR above 79.28 dB, compared to other related works.

Article Highlights

- Developing a medical image watermarking approach to secure sensitive patient information.
- Introducing new directions to enhance the robustness and imperceptibility of the watermark against various kinds of attacks.
- Achieving high performance in the embedding and extraction processes.

Keywords Medical image security · Discrete wavelet transform · Singular value decomposition · Robustness · Imperceptibility · Firefly algorithm

✉ Waleed Alomoush, waleed.alomoush@skylineuniversity.ac.ae | ¹School of Computing, Skyline University College, P.O. Box 1797, Sharjah, United Arab Emirates. ²Research and Innovation Centres, Rabdan Academy, P.O. Box 114646, Abu Dhabi, United Arab Emirates. ³Department of Computer Science and Computer Engineering, United Arab Emirates University, Al Ain, Abu Dhabi, UAE. ⁴Faculty of Information Technology, Applied Science Private University, Amman 11931, Jordan. ⁵AI Center for Precision Health, Weill Cornell Medicine-Qatar, Doha, Qatar. ⁶Department of Artificial Intelligence, College of Information Technology, Misr University for Science and Technology (MUST), 6th of October City 12566, Egypt.



1 Introduction

Telemedicine is a rapidly growing field in clinical medicine, used to transmit patients' medical information across interactive media for consultations and remote medical examinations. For instance, digital medical imaging and communication in medicine (DICOM) are employed to transfer medical image reports (such as CT, and X-ray imaging) through networks. Medical images are also considered vital tools for doctors' decision-making. Thus, the security of these images is regarded as critical in the telemedicine process, making robust protection systems for these images essential [1, 2].

Digital image copyright and authentication are key issues due to the high demand for image-processing tools that modify image content, data collection, and data protection [3, 4]. An image security system is essential for protecting images from unauthorized access and attacks when transferred across public networks [1, 5]. The medical image watermarking security system has been confirmed as one of the most commonly utilized protection systems for authorization and copyright protection that prevents violations of medical image content. This system embeds a watermark into the host image through a specific mechanism that can be extracted or detected later (after data reception) without causing any distortion to the protected image [6].

Embedded watermarking imperceptibility and robustness are considered the main criteria for the watermarking process, which must protect the embedded watermark from detection and removal by random or unexpected malicious attacks. However, robustness and imperceptibility are often conflicting objectives in evaluating watermarking mechanisms [7].

Watermarking can be classified into three categories depending on the mechanism parameters and conditions: semi-fragile, fragile, and robust [8]. Robust image watermarking protects images from expected attacks that attempt to destroy and remove the image watermark without significantly affecting the visual quality [9], typically applied for copyright rights and ownership verifications. In contrast, fragile watermarking is utilized to ensure credibility and image validity, rather than verifying ownership authenticity. Fragile watermarking aims to detect any unauthorized changes or damage caused by minor interferences or modifications to the watermarked image. Semi-fragile watermarking combines the characteristics of robustness and fragility while maintaining robustness against permitted manipulations and is often used for authentication [8, 10]. Several approaches have been introduced to incorporate watermarks into the frequency domain, often employing various transformations such as SVD, DWT, A discrete Fourier transform (DFT), discrete cosine transform (DCT), and integration methods like DWT–SVD, DCT–SVD, and DCT–DWT Wavelet transformation is recognized as one of the most effective techniques for achieving a balance between transparency and robustness. The robustness and imperceptibility of the watermarking methods are enhanced through the integration of SVD and DWT [7].

Modifications to the embedding watermark for host images can be made using certain watermarking methods. It is crucial to determine the volumes of adjustments needed to achieve a reasonable tradeoff between robustness and imperceptibility. These modification volumes are usually set by variables known as strength factors. Consequently, to determine the best strength factors, an effective and efficient algorithm is required to optimize the tradeoff between imperceptibility and robustness [3, 7, 11]. The primary objective of this study is to determine the optimal values of multiple strength factors (MSFs). The optimization of the best MSFs is addressed using heuristic methods.

This paper presents an image watermarking integration method using DWT and SVD, where the optimal values of MSFs are determined by the firefly Photinus algorithm (FPA) to balance robustness and imperceptibility. The LL3 sub-band singular values of the host image are embedded as singular values using MSFs. A linear combination of the peak signal-to-noise ratio (PSNR) and normal correlation coefficient (NC) is used as an objective function in this research. The remainder of this paper is organized as follows: Sect. 2 introduces related work on the integration of DWT- and SVD-based meta-heuristic search algorithms for image watermarking. Section 3 presents the FA, and Sect. 4 introduces the FPA algorithm. The integration process between the DWT and SVD is presented in Sect. 5. The proposed DWT–SVD-FPA method is detailed in Sect. 6. The experiments and results are discussed in Sect. 7, which also concludes the paper.

2 Literature review

In the field of medical image security, few efforts have been reported in recent years focusing on developing medical image watermarking mechanisms using meta-heuristic search optimization algorithms, which are considered a preferable choice for such problems. These algorithms are used to determine the optimal value of MSFs in watermarking

methods, which have significantly improved outcomes [7, 12–14]. This section is divided into three subsections: first, we review studies of medical image watermarking using FAs; second, we review studies of medical image watermarking mechanisms based on other meta-heuristic search optimization algorithms; and third, we discuss the main contribution of this work.

2.1 Medical image watermarking based on firefly algorithm

Moeinaddini and Afsari [7] introduced a new DWT–SVD optimized watermarking approach using a modified FA based on opposition and dimensionality (ODFA). The experiments and outcomes of the proposed approach demonstrate a good degree of robustness and imperceptibility compared with other state-of-the-art methods.

The FA has recently been used by researchers to establish optimal trade-offs between robustness and imperceptibility in image watermarking techniques. Mishra et al. [8] The FA has recently been used by researchers to establish optimal trade-offs between robustness and imperceptibility in image watermarking techniques. Dong et al. [11] employed a chaotic FA to determine the optimal values of MSFs in the DCT-SVD domain; this method was used for grayscale image watermarking. The outcomes of the approach presented in [10] also showed that the proposed method was superior in terms of imperceptibility and robustness compared to other related works.

Kazemivash and Moghaddam [15] introduced a grayscale image watermarking approach that utilizes the Lifting Wavelet Transform (LWT) based on the FA to select appropriate watermark blocks for embedding in the host image. Additionally, Kazemivash and Moghaddam [16] presented another watermarking mechanism employing the FA method, which depends on the transformation of the lifting wavelet; here, the watermark in the host image is embedded using the expected regression tree value, with MSFs performed using FA. Although the method proposed in [16] achieved superior robustness, it did not adequately maintain the transparency of the host image.

2.2 Medical image watermarking based other *meta*-heuristic algorithms

Ali et al. [12] Introduced a watermarking mechanism based on the ABC algorithm and a fixed distribution using DWT–SVD. In this research, the ABC algorithm was used to optimize the values of MSFs. Furthermore, Lai [17] employed SVD based on a tiny genetic algorithm to determine the best MSF values, while Ishtiaq et al. [18] used particle swarm optimization (PSO) to find the optimal MSF values in the domain of DCT. The authors used the PSNR criterion to evaluate the strength, which was used as the objective function. Loukhaoukha et al. [13] utilized the Ant Colony Optimization algorithm with multiple objectives in the domain of LWT-SVD to determine the best MSF values.

Sankaran et al. [19] proposed a new approach to achieve distortion-free watermarking using a method subject to pixel weight. The main idea of this approach was to improve performance and security using a two-level DWT to identify the optimal embedding region with a dragonfly optimization algorithm. Verma and Sharma [20] proposed a method that generates better results for medical images using various invisible watermarking approaches, including transformation and frequency domains; the proposed approach is a hybrid method that combines two merging methods.

Anand and Singh [21] proposed an improved watermarking approach with the capacity to protect patient data using multiple watermarks embedded in the domain of medical images by DWT–SVD. The Hamming code was used as a text watermark before the embedding process to reduce distortion from channel noise for sensitive data. The image watermark was encrypted and compressed post-embedding. The Chaotic-LZW combination demonstrated the highest effectiveness among the various encryption methods, and three compression systems were evaluated.

Kahlessenane et al. [1] proposed a blind watermarking approach that allows a patient's record to be combined into a computed tomography image scan. In this approach, DWT was applied to the medical images before the combination process, followed by the topological reorganization of the LL sub-band coefficients using zigzag scanning. The watermarked bits were then integrated when the combination process of coefficients was completed. This watermark combination process can be easily verified when a patient's hash record is integrated into medical images.

Swaraja et al. [22] Proposed a method for the region of non-interest (RONI) using dual watermarks to conceal medical image blocks within the RONI, which is used to detect tampering through authenticity and recognition. These blocks were selected using DWT features aligned with the human visual system (HVS) and the particle swarm bacterial foraging optimization algorithm (PSBFO). The threshold value for achieving optimal outcomes was chosen using the PSBFO algorithm, which led to the best robustness and imperceptibility. Moreover, the Lempel–Ziv lossless compression method was used to compress the dual watermarks to enhance payload capacity.

Balasamy et al. [23] conducted several studies using an adaptive neuro-fuzzy model and an integrated watermark transformation mechanism based on the region of interest (ROI), which was employed to identify regions of medical imaging that reflect high-energy intensity levels. Furthermore, wavelet decomposition was used to extract the sub-bands for embedding [24, 25]

2.3 Discussions and main contributions of this work

Table 1 summarizes the advantages and disadvantages of each reviewed method, highlighting the main limitations of each approach. It is evident from Table 1 that many of the approaches presented are limited in terms of robustness and maintaining image transparency.

In the proposed approach, the optimal values of MSFs are determined by the FPA to balance robustness and imperceptibility. The capability of the FPA is enhanced, which leads to an increase in the strength of robustness and imperceptibility. The proposed approach demonstrates good similarity between the host and watermarked images, strong robustness against various image-processing operations and attacks, and well-maintained image transparency.

3 Firefly algorithm

Yang [26] Proposed a meta-heuristic search algorithm called the FA, inspired by the behavior of fireflies and the flash signals they use to attract potential mates. The attractiveness of a firefly depends on the intensity of its flash; thus, a firefly is attracted to another firefly that exhibits higher brightness, moving towards it. The flash intensity, which directly influences the value of the objective function, is computed using Eq. 1:

$$I(r) = I_0 e^{-\gamma r^2} \quad (1)$$

where the light source intensity is represented by I_0 , the flash absorption coefficient is γ , and the distance between the fireflies is r . The attractiveness of the firefly β can be computed using the equation as follows:

$$\beta(r) = \beta_0 e^{-\gamma r^2} \quad (2)$$

The attractiveness is represented by β_0 when the distance is 0. The distance r between fireflies i and j can be computed using the following equation:

$$r_{ij} = \sqrt{\sum_{k=1}^n (z_{ik} - z_{jk})^2} \quad (3)$$

The dimension of the problem is n . Each firefly moves toward another firefly using the following equation:

$$z_i(t+1) = z_i(t) + \beta_0 e^{-\gamma r_{ij}^2} (z_j(t) - z_i(t)) + \alpha \varepsilon_i \quad (4)$$

where ε_i is a random number between 0–1. Also, the movement of fireflies is affected by using the following three factors: the current firefly position, suitability to another firefly position, and random constraint values α and ε_i . The main steps of the FA can be summarized as follows (Fig. 1).

4 Firefly *Photinus* algorithm

Alomoush et al. [27] proposed a new version of the FA, called the FPA, which introduces a mate list mechanism to address problems such as remembering history and being trapped in local optima. The FPA also proposes a new absorption coefficient (σ) that changes with time to solve the issue of static parameters. The main steps of the FPA are summarized in the pseudocode shown in Fig. 2.

In addition, new modifications to the FPA were used to solve problems associated with the original FA, such as fixed FA parameters, the memory of any situation, and avoiding becoming stuck in local optima. These modifications are discussed below.

Table 1 Summary of image watermarking mechanisms based on meta-heuristic search optimization algorithms

	Approach	Advantages	Disadvantages
1	Moeinaddini and Afsari [7]	Good degree of imperceptibility and robustness	Limited robustness against rotation and cropping
2	Mishra et al. [8]	The embedding and extraction of the proposed algorithm are well optimized	Image transparency is not well maintained
3	Dong et al. [10]	Good imperceptibility	Limited robustness
4	Kazemivash and Moghaddam [16]	Uses FA to optimize multi-scaling factor significantly influencing imperceptibility and robustness	Transform domain with rotation invariant
5	Ali et al. [12]	Competitively in terms of imperceptibility and robustness	Scheme is free from false positive detection problems
6	Kahlessenane, Khaldi [1]	Good degree of imperceptibility and robustness	The watermarked image must resist various attacks to preserve watermark integrity
7	Sankaran, Rayna [19]	Good degree of imperceptibility	Limited robustness
8	Anand and Singh [21]	Robustness for various attacks while maintaining imperceptibility	Image transparency is not well maintained

```

/* Initialization of Population
1 Initialize the population of fireflies ( $N$ ) and generate solutions  $x_i, i=1, 2, \dots, N$ ;
2 For each firefly, compute the fitness value;
3  $t = N$ ;
4 While ( $t < \text{MaxGeneration}$ ) do
5     |
6     |   For  $i=1$  to  $N$  do
7     |   |   For  $j=1$  to  $N$  do
8     |   |   |   if  $I_j > I_i$  then
9     |   |   |   |   According to Eq. 4 Move firefly  $X_i$  toward  $X_j$ ;
10    |   |   |   |   Compute the value of fitness for a new solution;
11    |   |   |   |    $t++$ ;
12    |   |   |   end
13    |   |   end
14    |   end
15 end

```

Fig. 1 Firefly algorithm

```

/* Initialization of Population
1 Initialize the population of fireflies ( $N$ ) and generate solutions  $x_i, i=1, 2, \dots, N$ ;
2 Set the new absorption coefficient  $\sigma$ 
3 Initialize mate  $\{M\}$  as a list.
4 For each firefly, compute the fitness value;
5  $t = N$ ;
6 While ( $t < \text{MaxGeneration}$ ) do
7     |
8     |   For  $i=1$  to  $N$  do
9     |   |   For  $j=1$  to  $N$  do
10    |   |   |   if  $I_j > I_i$  and ( $i$  mate  $j \notin \{M\}$ ) then
11    |   |   |   |   According to Eq. 4 Move firefly  $X_i$  toward  $X_j$ ;
12    |   |   |   |   Update mate list  $\{M\}$ 
13    |   |   |   |   Compute the value of fitness for a new solution;
14    |   |   |   |   According to Eq 6. Update absorption coefficient  $\gamma$  based
15    |   |   |   |    $\sigma$ 
16    |   |   |   |    $t++$ ;
17    |   |   |   end
18    |   |   end
19    |   end
20 end

```

Fig. 2 Firefly Photinus algorithm

4.1 Update mate list

In each iteration of the FPA, the movement process generates a new position as a solution, which is then stored in a mate list M as shown in Eq. 5:

$$\{M_{t+1}\} = \{M_t\} - \{x_i^{t-6}\} + \{x_i^{t+1}\} \quad (5)$$

The new position for firefly i , is x_i^{t+1} when forwarding to j , where t is the time iteration, and $\{M_{t+1}\}$ is the new status of the mate list after the next movement to generate a new solution. It is important to note that when a new position is stored in the M list, firefly i is not allowed to move or revisit this position until it is removed from the mate list after a suitable number of movements, depending on the mate list size. See Fig. 3.

Fig. 3 FPA mate list

M_1	x_i^1						
M_2	x_i^2	x_i^1					
M_3	x_i^3	x_i^2	x_i^1				
.....							
M_7	x_i^7	x_i^6	x_i^5	x_i^4	x_i^3	x_i^2	x_i^1
M_8	x_i^8	x_i^7	x_i^6	x_i^5	x_i^4	x_i^3	x_i^2
.....							
M_{t+1}	x_i^{t+1}	x_i^t	x_i^{t-1}	x_i^{t-2}	x_i^{t-3}	x_i^{t-4}	x_i^{t-5}

4.2 New absorption coefficient (σ)

The absorption coefficient parameter gamma (γ) remains fixed in FA during the iteration time, whereas in FPA, the value of γ changes during the iteration time according to the new absorption coefficient sigma (σ). Equation 6 shows the relationship between γ and σ during the iteration.

$$\gamma(t + 1) = \sigma \cdot \gamma(t) \tag{6}$$

where $0 < \sigma \leq 1$ and it controls the dominance area of the firefly intensity through the iteration time, as shown in Eq. 7.

$$\text{when } 0 < \sigma \leq 1 \Rightarrow \begin{cases} \gamma(t + 1) \leq \gamma(t) \\ \beta(t + 1) \geq \beta(t). \end{cases} \tag{7}$$

5 DWT-SVD-based watermarking algorithm

This paper investigates the effects of scaling factors (SFs) on the values of normalized cross-correlation (NC) for the original watermark (W) and the recovered watermarks (W'), and peak signal-to-noise ratio (PSNR). PSNR is used to determine the visual quality of the signed images, as shown in Eq. 8:

$$PSNR = 10 \log_{10} \left(\frac{I_{max}^2}{MSE} \right) \tag{8}$$

where MSE represents the Mean Square Error, and I_{max} is the maximum possible pixel value for image I .

Initially, the watermark is extracted, and then $NC(W, W')$ is computed using Eq. 9:

$$NC(W, W') = \frac{\sum_{i=1}^m \sum_{j=1}^n [W(i, j) \cdot W'(i, j)]}{\sum_{i=1}^m [W(i, j)]^2} \tag{9}$$

5.1 Watermark embedding algorithm

The proposed watermarking scheme employs a watermark W of size $m \times m$, and a host image I of size $N \times N$, embedded as follows (Fig. 4).

-
- 1 A HAAR filter applying a 3-level DWT is used on image I to isolate the sub-band LL3 of size $m \times m$.
 - 2 SVD is performed on the LL3 sub-band of the host image I as achieved in step 1 using Equation 10 to obtain S .

$$[U, S, V] = SVD(LL3) \quad (10)$$
 - 3 The singular values (S_w) are identified and SVD is performed on W as described in Equation 11.

$$[U_w, S_w, V_w] = SVD(W) \quad (11)$$
 - 4 Equation 12 is used to embed S_w into S values.

$$S' = S + \delta * S_w \quad (12)$$
 - 5 Changes in the LL3 sub-band are calculated as shown in Equation 13.

$$LL3' = U * S' * V^T \quad (13)$$
 - 6 To achieve the signed image I' , a 3-level Inverse DWT (IDWT) is performed.
-

Fig. 4 The embedded watermark algorithm

-
- 1 A HAAR filter applying a 3-level DWT is used on both the host image I and the signed image I' to achieve the sub-bands LL3 and LL3', where I' , and I are the same size of $m \times m$.
 - 2 SVD is performed on the sub-bands LL3 and LL3' using Equations 10 and 14 to obtain the singular values S and S' .

$$[U', S', V'] = SVD(LL3') \quad (14)$$
 - 3 Equation 15 is used to calculate the singular values.

$$S'_w = (S' - S) / \delta \quad (15)$$
 - 4 Equation 16 is used to recover the extracted watermark image.

$$W' = U_w * S'_w * V_w^T \quad (16)$$
-

Fig. 5 The watermark extraction algorithm

5.2 Watermark extraction algorithm

Watermark extraction is performed by employing the signed image's DWT-SVD mechanisms. Figure 5 illustrates the watermark extraction algorithm.

6 Proposed approach (DWT-SVD-FPA)

In this study, a new watermarking mechanism using the combination of DWT and SVD based on the FPA, termed DWT-SVD-FPA, is proposed. The FPA is implemented to optimize the values of MSF, δ . The best FPA outcomes are computed using the objective function shown in Eq. 17.

$$f(x) = PSNR + \varphi * \left[NC(W, W') + \sum_{i=1}^T NC(W, W'_i) \right] \quad (17)$$

where $NC(W, W')$, and $NC(W, W'_i)$ are the cross-correlation between the original and recovered watermarks from the signed image, and each attacked signed image, respectively. The values of NC include a weighting factor ϕ , and the DWT-SVD-FPA is represented as follows (Fig. 6).

Fig. 6 The proposed approach algorithm (DWT–SVD-FPA)

1	Set n Firefly Photinus randomly, where each i that belongs to n is a row vector of size $m \times m$.
2	For each photinus i of the population, perform the following processes: <ol style="list-style-type: none"> i. Execute the watermark embedding algorithm (Algorithm 3) using Equation 13, where δ is the MSF achieved by FPA. ii. Apply image-processing attacks T to the signed image I'. iii. Extract the watermarks from the attacked watermarked images using the algorithm (Algorithm 4). iv. Calculate the values of PSNR between I and I', and NC (W, W') for the attacked images. v. Compute the $f(x)$ value of the firefly by the objective function as in Equation 17.
3	Move the Firefly Photinus according to the steps in (Algorithm 2).
4	Repeat: Continue repeating steps 2 and 3 until the maximum number of generations ($MaxGeneration$) is reached.

The value of NC is much smaller than PSNR; therefore, a weighting factor ϕ is used in Eq. 17 to balance out the resulting effects.

7 Experimental results and discussion

This section evaluates and discusses the performance of the DWT–SVD-FPA. The experiments were conducted on medical image databases introduced in [28], which include tomography scanned images with dimensions of 512×512 , as shown in Fig. 7. Setting proper algorithm parameters is considered critical; indeed, to achieve a fair comparison between the

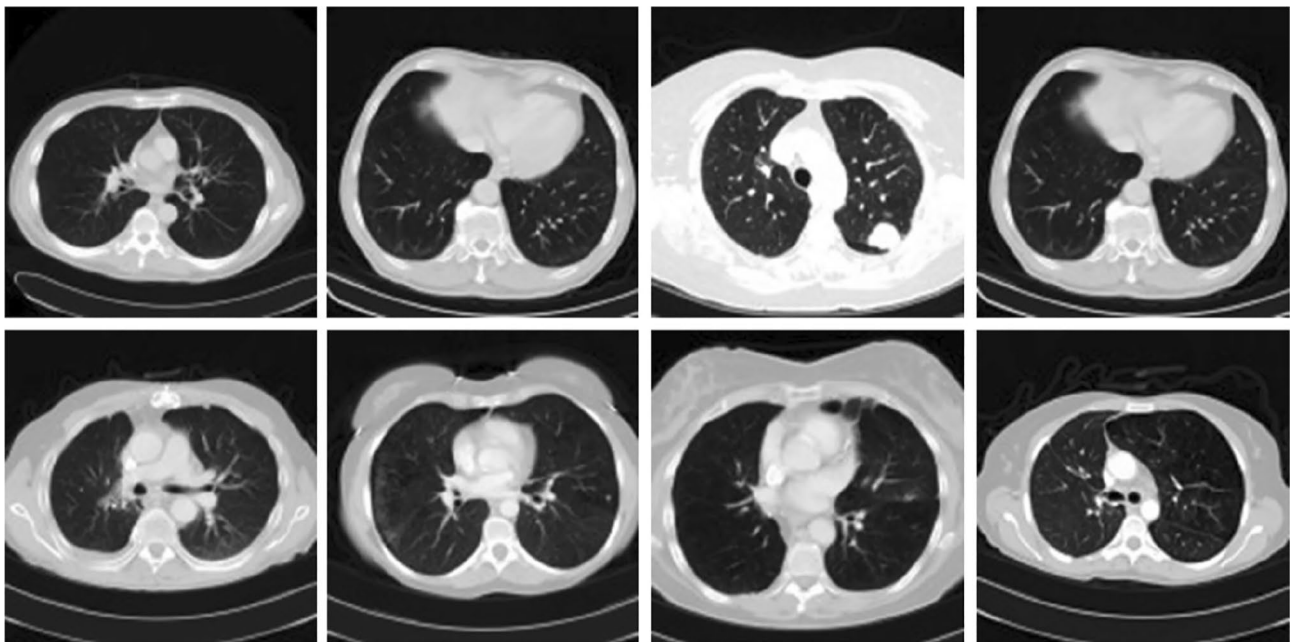


Fig. 7 Medical images datasets [28]

proposed approach and other related works, it is important to ensure an apples-to-apples comparison. In these experiments, the parameters of the proposed DWT–SVD-FPA watermarking algorithm were set based on other related works, such as DWT–SVD-FA [8], and FPA introduced in [27], which were set as follows: $\beta_0 = 1$, $\alpha = 0.01$, $\gamma = 1.0$, $M = 7$, $\sigma = 0.95$, $n = 10$, $\phi = 10$, and number of the iterations $ML = 10$.

Table 2 shows the proposed DWT–SVD-FPA algorithm values for NC and PSNR values of the proposed algorithm (DWT–SVD-FPA) compared to the watermarking schema-based original FA, named DWT–SVD-FA.

The outcomes of Table 2 show that the proposed algorithms, DWT–SVD-FPA and DWT–SVD-FA, have acceptable imperceptibility because their minimum values are 0.989 and 72.35 dB, respectively. Moreover, the average NC value of the DWT–SVD-FPA outperforms that of the DWT–SVD-FA and provides better robustness against attacks as a result of the capability to fine-tune multiple scaling values via the meta-heuristic algorithm of the FPA.

In addition, to evaluate the imperceptibility of the proposed DWT–SVD-FPA, the obtained PSNR values were compared with those reported in [1, 20, 21, 29]. Table 3 illustrates that the PSNR performance rates of the proposed DWT–SVD-FPA are satisfactory compared to state-of-the-art methods at an integration value of 100%.

Table 4 presents the NC outcomes for the CT-scanned images obtained by the proposed DWT–SVD-FPA algorithm, where eight different image-processing operation attacks were applied to assess robustness. These attacks include histogram equalization, Gaussian noise, sharpening, JPEG compression, average filtering, cropping, salt-and-pepper noise, and scaling.

As shown in Table 4, the proposed DWT–SVD-FPA algorithm outperforms other related works based on various attacks, such as histogram equalization, sharpening, JPEG compression, average filtering, and scaling. However, its performance is slightly lower for Gaussian noise, salt-and-pepper noise, and cropping. Table 4 also confirms that the robustness achieved by the proposed DWT–SVD-FPA is improved through the application of the FPA, which determines the optimal MSF value. The FPA implements a linear combination of the NC (W, W_0) objective function for the signed and attacked images. Furthermore, the PSNR of the signed image was calculated for these eight attacks. The obtained values of NC (W, W_0) ranged from 0 to 0.04, indicating high robustness.

Finally, Table 4 demonstrates that the proposed DWT–SVD-FPA algorithm retains good perceptible image quality for the signed and attacked images. Therefore, the conclusion is that the visual quality and robustness criteria are effectively met in the DWT–SVD-FPA approach, which is justified by the improvement in MSFs resulting from the embedding of the FPA.

8 Conclusion

This study proposes a medical image watermarking integration method that employs DWT and SVD. The optimal values of MSFs are determined by the FPA, which achieves a valuable balance between robustness and imperceptibility. The LL3 sub-band singular values of the host image are embedded using these MSFs, and a linear combination of PSNR and NC is used as the objective function in this research. The DWT–SVD-FPA was applied to CT images, and eight different image-processing operations were used to test the robustness of the proposed algorithm: histogram equalization, Gaussian noise, sharpening, average filtering, cropping, JPEG compression, salt-and-pepper noise, and scaling. The performance of the proposed algorithm indicates significant improvements in the embedding and extraction processes, as well as in the balance between robustness and imperceptibility compared to other related works. The limitations of this work include issues with the DWT, such as its phase sensitivity and lack of directionality, which can be potentially addressed

Table 2 The PSNR and NC (W, W') Outcomes of (DWT–SVD-FPA) and (DWT–SVD-FA)

Integration (%)	DWT–SVD-FPA		DWT–SVD-FA		
	NC (W, W')	PSNR (db)	NC (W, W')	PSNR	
10		156.20	1	145.96	1
20		142.74	1	140.30	1
30		129.03	1	118.51	1
40		107.10	1	100.82	1
50		103.96	1	94.88	0.989
70		90.16	1	91.07	0.990
100		79.28	1	72.35	0.992

Table 3 Comparison of the PSNR values of the proposed DWT-SVD-FPA algorithm and related work

	DWT-SVD-FPA	DWT-SVD-FA	Kahlessenane et al. [1]	Anand and Singh [21]	Verma and Sharma [20]	Thakkar and Srivastava [29]
PSNR (dB)	79.28	72.35	74.47	44.19	63.67	56.69

Table 4 Comparison of NC outcomes of the proposed DWT–SVD–FPA algorithm and related work

	DWT–SVD–FPA	DWT–SVD–FA	Kahlessenane et al. [1]	Anand and Singh [21]	Verma and Sharma [20]	Thakkar and Srivastava [29]
Histogram equalization	0.9882	0.9695	0.9782	0.7223	–	0.9678
Gaussian noise	0.9790	0.9741	0.9633	0.9803	0.9208	0.9632
Sharpening	1.0000	0.9863	0.9873	0.6506	–	0.9900
Average filtering	0.9956	0.9800	0.9708	0.9860	0.8380	0.9434
Cropping	0.7794	0.7251	0.7818	0.3586	0.6516	0.7120
JPEG Compression	0.9580	0.9330	0.9238	0.9388	–	0.8378
Salt-and-pepper noise	0.9786	0.9573	0.9715	0.9251	0.9817	0.9657
Scaling	0.9604	0.9362	0.9175	0.7157	0.7142	0.9073

by exploring alternative transforms, such as the Complex Wavelet Transform or Redundant DWT (RDWT). Future work will focus on enhancing robustness against these attacks and generalizing this approach to color images and videos.

Author contributions Methodology, WA (Waleed Alomoush) and OAK (Osama A. Khashan); Software, WA and MA (Mohammad Alshinwan); Validation, AA (Ayat Alrosan) and; Formal analysis, RD (Rafat Damseh) Resources OAK, AA, Data curation, MA and AAA (Alaa Ali Abd-Alrazaq) Writing—original draft, RD, AAA and MD (Mohanad A.Deif); Writing—review and editing, AA, M., Visualization, Supervision, OAK and WA; Project administration, WA and all authors have read and agreed to the published version of the manuscript.

Funding The authors would like to acknowledge Rabdan Academy for its support of this work.

Data availability This study is used benchmark dataset, which are available online repository and its mention in the references.

Declarations

Competing interests The authors declare no competing interests.

Open Access This article is licensed under a Creative Commons Attribution 4.0 International License, which permits use, sharing, adaptation, distribution and reproduction in any medium or format, as long as you give appropriate credit to the original author(s) and the source, provide a link to the Creative Commons licence, and indicate if changes were made. The images or other third party material in this article are included in the article's Creative Commons licence, unless indicated otherwise in a credit line to the material. If material is not included in the article's Creative Commons licence and your intended use is not permitted by statutory regulation or exceeds the permitted use, you will need to obtain permission directly from the copyright holder. To view a copy of this licence, visit <http://creativecommons.org/licenses/by/4.0/>.

References

- Kahlessenane F, Khaldi A, Kafi R, Euschi S. A DWT based watermarking approach for medical image protection. *J Ambient Intell Hum Comput*. 2020. <https://doi.org/10.1007/s12652-020-02450-9>.
- Favorskaya M, Savchina E, Gusev K. Feature-based synchronization correction for multilevel watermarking of medical images. *Procedia Comput Sci*. 2019;159:1267–76.
- Zhou X, Zhang H, Wang C. A robust image watermarking technique based on DWT, APDCBT, and SVD. *Symmetry*. 2018;10(3):77.
- Alomoush W, Khashan OA, Alrosan A, Attar HH, Almomani A, Alhosban F, et al. Digital image watermarking using discrete cosine transformation based linear modulation. *J Cloud Comput*. 2023;12(1):1–17.
- Du L, Ho AT, Cong R. Perceptual hashing for image authentication: a survey. *Signal Process: Image Commun*. 2020;81:115713.
- Begum M, Uddin MS. Digital image watermarking techniques: a review. *Information*. 2020;11(2):110.
- Moienaddini E, Afsari F. Robust watermarking in DWT domain using SVD and opposition and dimensional based modified firefly algorithm. *Multim Tools Appl*. 2018;77(19):26083–105.
- Mishra A, Agarwal C, Sharma A, Bedi P. Optimized gray-scale image watermarking using DWT–SVD and Firefly Algorithm. *Expert Syst Appl*. 2014;41(17):7858–67.
- Ansari IA, Pant M, Ahn CW. Artificial bee colony optimized robust-reversible image watermarking. *Multim Tools Appl*. 2017;76(17):18001–25.
- Soualmi A, Alti A, Laouamer L. A new blind medical image watermarking based on weber descriptors and Arnold chaotic map. *Arab J Sci Eng*. 2018;43(12):7893–905.
- Dong H, He M, Qiu M. Optimized gray-scale image watermarking algorithm based on DWT–DCT–SVD and chaotic firefly algorithm. In: 2015 International Conference on cyber-enabled distributed computing and knowledge discovery. IEEE; 2015. pp. 310–3.

12. Ali M, Ahn CW, Pant M, Siarry P. An image watermarking scheme in wavelet domain with optimized compensation of singular value decomposition via artificial bee colony. *Inf Sci.* 2015;301:44–60.
13. Loukhaoukha K, Chouinard J-Y, Taieb MH. Optimal image watermarking algorithm based on LWT-SVD via multi-objective ant colony optimization. *J Inf Hiding Multim Signal Process.* 2011;2(4):303–19.
14. Wang Y-R, Lin W-H, Yang L. An intelligent watermarking method based on particle swarm optimization. *Expert Syst Appl.* 2011;38(7):8024–9.
15. Kazemivash B, Moghaddam ME. A robust digital image watermarking technique using lifting wavelet transform and firefly algorithm. *Multim Tools Appl.* 2017;76(20):20499–524.
16. Kazemivash B, Moghaddam ME. A predictive model-based image watermarking scheme using Regression Tree and Firefly algorithm. *Soft Comput.* 2018;22(12):4083–98.
17. Lai C-C. A digital watermarking scheme based on singular value decomposition and tiny genetic algorithm. *Digit Signal Process.* 2011;21(4):522–7.
18. Ishtiaq M, Sikandar B, Jaffar MA, Khan A. Adaptive watermark strength selection using particle swarm optimization. *ICIC Express Lett.* 2010;4(5):1–6.
19. Sankaran KS, Rayna HA, Mangu V, Prakash V, Vasudevan N. Image water marking using DWT to encapsulate data in medical image. In: 2019 International conference on communication and signal processing (ICCSP). IEEE; 2019. pp. 0568–71.
20. Verma U, Sharma N. Hybrid mode of medical image watermarking to enhance robustness and imperceptibility. *Int J Innov Technol Explor Eng.* 2019;9:351–9.
21. Anand A, Singh AK. An improved DWT-SVD domain watermarking for medical information security. *Comput Commun.* 2020;152:72–80.
22. Swaraja K, Meenakshi K, Kora P. An optimized blind dual medical image watermarking framework for tamper localization and content authentication in secured telemedicine. *Biomed Signal Process Control.* 2020;55:101665.
23. Balasamy K, Krishnaraj N, Vijayalakshmi K. An adaptive neuro-fuzzy based region selection and authenticating medical image through watermarking for secure communication. *Wirel Pers Commun.* 2022;122(3):2817–37.
24. Balasamy K, Krishnaraj N, Vijayalakshmi K. Improving the security of medical image through neuro-fuzzy based ROI selection for reliable transmission. *Multim Tools Appl.* 2022;81(10):14321–37.
25. Suganyadevi S, Seethalakshmi V, Balasamy K. A review on deep learning in medical image analysis. *Int J Multim Inf Retr.* 2022;11(1):19–38.
26. Yang X-S. Firefly algorithm, stochastic test functions and design optimisation. 2010. [arXiv:1003.1409](https://arxiv.org/abs/1003.1409).
27. Alomoush W, Omar K, Alrosan A, Alomari YM, Albashish D, Almomani A. Firefly Photinus search algorithm. *J King Saud Univ – Comput Inf Sci.* 2018. <https://doi.org/10.1016/j.jksuci.2018.06.010>.
28. Mader K. CT images from cancer imaging archive with contrast and patient age. 2017. <https://www.kaggle.com/kmader/siim-medicalimages>.
29. Thakkar FN, Srivastava VK. A blind medical image watermarking: DWT-SVD based robust and secure approach for telemedicine applications. *Multim Tools Appl.* 2017;76(3):3669–97.

Publisher's Note Springer Nature remains neutral with regard to jurisdictional claims in published maps and institutional affiliations.